

# Morphology, strength and pre-coating effect in YSZ/Ni bonding

J. G. DUH, Y. C. WU

*Department of Materials Science and Engineering, National Tsing Hua University, Hsinchu, Taiwan*

B. S. CHIOU

*Institute of Electronics, National Chiao Tung University, Hsinchu, Taiwan*

The quality of ceramic-metal bond is strongly influenced by the microstructure of the transition region between the ceramic and the metal. Sandwich-like ceramic-metal-ceramic specimens are fabricated by solid state bonding of 3 mol% yttria doped zirconia ceramic with nickel foils. Time dependence of the shear strength of the bonding assembly is evaluated at 900°C under a bonding pressure of 8.17 MPa. An optimum strength is obtained for the bonding time between 10 and 25 minutes. The shear strength is also measured as the function of the bonding pressure and bonding temperature. The dependence of the processing parameters on the shear strength of the bond assembly is investigated on the basis of the morphological development in the ceramic-metal interface. In addition, the effect of a pre-coated Ni film on the strength of YSZ/Ni bonding is discussed.

## 1. Introduction

The technique of ceramic-metal bonding is an important consideration in the fabrication and application of high temperature structural ceramics [1, 2]. Ceramic-metal interfaces represent a critical part in material joint processing.  $ZrO_2$ -Ni is a model system in the investigation of composite materials made by bonding ceramics and metals [3-7]. Partially-stabilized zirconia (PSZ) has attracted a lot of attention for the superior thermal shock-resistance, high strength and toughness. Nickel is one of the base metals for the high temperature alloys.

The purpose of this study is to investigate the solid state bonding between 3 mol% yttria stabilized zirconia (YSZ3) and nickel. YSZ3 is chosen for its high fracture toughness, which is nearly unaffected by the thermal cycling [8]. In this study, sandwich-like ceramic-metal-ceramic specimens are fabricated by solid state bonding of yttria doped zirconia ceramic with the nickel foil. The shear strength of the bonding is evaluated in terms of several controlling parameters including the bonding pressure, bonding time and bonding temperature. The morphological development of the ceramic-metal interface is obtained with the aid of scanning electron microscope and electron microprobe. The variation in the shear strength as the function of the controlling parameter will be discussed with respect to the morphological development associated with the ceramic-metal interfacial microstructure.

## 2. Experimental Procedure

The zirconia selected for this study was YSZ3, i.e. zirconia doped with 3 mol% yttria (Toyo Soda Co.,

Tokyo, Japan). The chemical compositions of YSZ3 are listed in Table I. Samples of YSZ3, with 7.70 mm in diameter and 3.58 mm in thickness, were prepared by sintering at 1500°C for 1.5 h. The nickel samples with 8.10 mm in diameter and 0.05 mm in thickness were cut from 99.9% Ni foils.

Prior to bonding, the YSZ3 was polished and then cleaned ultrasonically in 60-80°C B.P. petroleum ether followed by 10%  $HNO_3$  in the ethanol solution. The specimen was then rinsed in water and allowed to air dry. As a final treatment, the YSZ was pre-baked to 1000°C for 3 h in air. It is believed that such a treatment would effectively clean the surface of any hydrocarbons remained after the solvent cleaning. The nickel foil was annealed at 1000°C for 2 h in vacuum to eliminate the effects of working and also to remove any hydrocarbons on the surfaces.

The YSZ3 discs and nickel foil were placed in a ceramic jig to hold them in alignment during the heating process. The bonding assembly was of sandwich type with the metal foil in between the ceramics. Fig. 1 shows the schematical representation of the bonding apparatus. The strength of the bonding assembly was evaluated in terms of the modulus of fracture by a shear test. The shear strength was measured in an Instron machine, and the cross head

TABLE I Chemical composition and characteristics of YSZ3

Y <sub>2</sub> O <sub>3</sub> (mol %)	ZrO <sub>2</sub> (mol %)	Average particle size (μm)	Specific surface area (m <sup>2</sup> /g)	Crystallite size (nm)
3	97	0.3	18	24

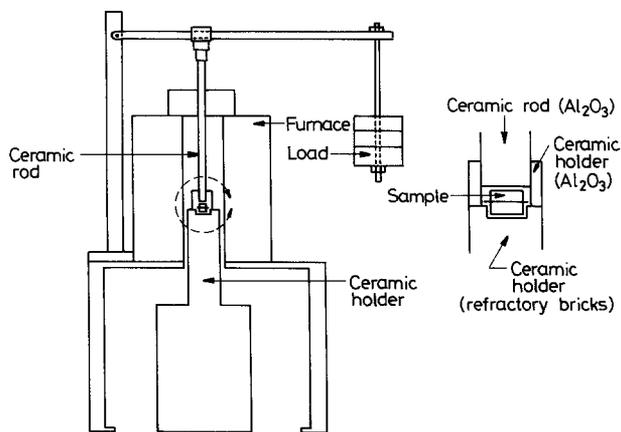


Figure 1 Schematic diagram of the bonding apparatus.

speed was set to be  $0.09 \text{ mm sec}^{-1}$ . The modulus of fracture were calculated by assuming a fully bonding interface between YSZ3 and Ni.

### 3. Results and Discussion

#### 3.1. Strength measurement and morphology in bonding

A series of bonding test were performed for the YSZ3–Ni–YSZ3 assembly at  $900^\circ\text{C}$  for various times ranging from 1 min to 90 min under a bonding pressure of 8.17 MPa. A reduced load of 4.4 MPa was applied during the cooling process after the bonding. Fig. 2 presents the time dependence of the shear strength. The bonding strength increases with the bonding time at the initial stage. Between 10 and 25 min, the bonding strength reaches a saturation value, and then it decreases continuously as the bonding time increases.

For most bonding assembly the fracture occurred at the nickel side of the nickel– $\text{ZrO}_2$  interface. The bonding strength in this study is measured with respect to this type of fracture. Fig. 3 indicates the X-ray diffraction pattern of the fracture surface. In addition to the original YSZ peaks, there are extra peaks shown up in Fig. 3, which is identified as NiO.

Fig. 4 shows the SEM micrograph and the profiles of X-ray intensities of zirconium and nickel in the vicinity of the bonding interface for the YSZ3–Ni–YSZ3 assembly bonded at  $900^\circ\text{C}$  for 5 min in air under a bonding pressure of 8.17 MPa. An intermediate layer, about  $3.5 \mu\text{m}$  thick, forms between YSZ3 and nickel. By combining the results of Figs 3 and 4, it is

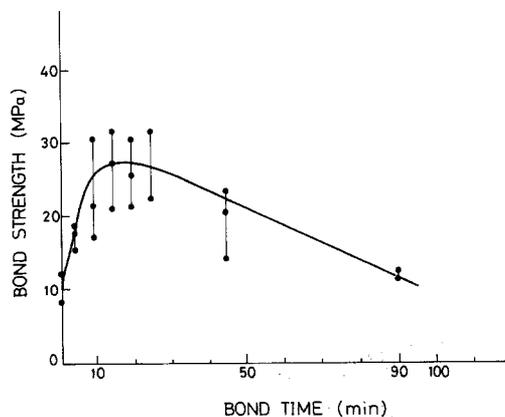


Figure 2 The time dependence of the shear strength bonded at  $900^\circ\text{C}$  under 8.17 MPa in air.

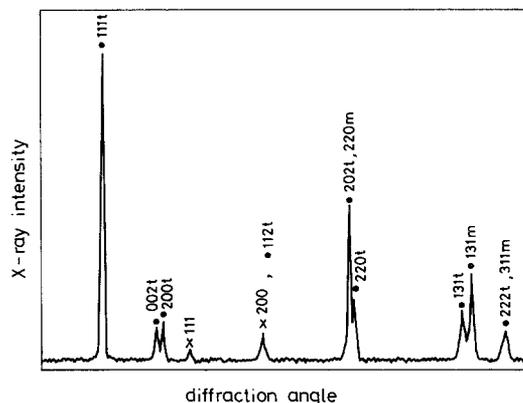


Figure 3 X-ray diffraction pattern for the fracture surface after bonding. (●)  $\text{ZrO}_2$ , (x) NiO.

argued that the intermediate layer contains the nickel oxide, NiO. The reaction between YSZ3 and the nickel oxide layer cannot be, however, revealed by scanning electron microscopy (SEM) or by electron microprobe (EPMA), which is also indicated in the work by Yamane and coworkers (4).

The bonding of Ni and YSZ3 mainly relies on the growth of NiO layer between them. At the beginning, the thickness of NiO layer is not sufficient to make a good contact with YSZ3, and the bonding strength is low. As the time increases, the growth of NiO layer is enhanced and this tends to increase the bonding strength. However, as the thickness of the NiO layer becomes larger, a stress develops between the materials with different thermal expansion coefficients. Table II lists the thermal expansion coefficients and elastic modulus of Ni, NiO and YSZ3. It appears that there is significant difference in thermal expansion coefficients between NiO and YSZ3. In addition to the introduced stress, the porous region, i.e., the voids between the Ni–NiO interface, also comes into effect. Fig. 5 represents the SEM micrographs in the vicinity of Ni–NiO interface bonded at  $900^\circ\text{C}$  under a pressure of 8.17 MPa for different bonding time. The thickness of NiO layer increases from  $3.7 \mu\text{m}$  for 5 min bonding to  $4.8 \mu\text{m}$  for 10 min and then  $8.5 \mu\text{m}$  for 15 min. The average porous region between Ni and NiO is estimated to be  $0.24 \mu\text{m}$ ,  $0.34 \mu\text{m}$  and  $0.48 \mu\text{m}$  for bonding time of 5, 10 and 15 min, respectively. It seems that the porous region enlarges as the time increases. By combination of the positive contribution of enhanced NiO growth and the negative effect of introduced stress and enlarged voids, the bonding strength would tend to reach a saturation value as indicated in Fig. 2. As the bonding time exceeds 30 min, the effects of introduced stress and the enlarged voids predominate, and the bonding strength tends to decline.

TABLE II The values of thermal expansion coefficients and elastic modulus of Ni, NiO and YSZ3

Sample	Ni	NiO	YSZ3
Thermal expansion coefficient ( $10^{-6} \text{ K}^{-1}$ )	17.6 ( $900^\circ\text{C}$ )	17.1	10.0 ( $1000^\circ\text{C}$ ) 8.0 (R.T.)
Elastic modulus (GPa)	205	277	201

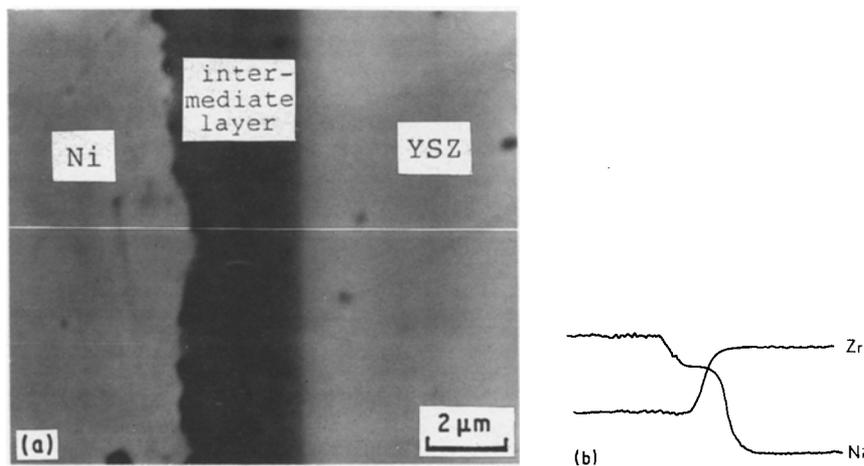


Figure 4 SEM micrograph and X-ray line profiles in the vicinity of the bonding interface (a) SEM micrograph, (b) X-ray profiles for Ni and Zr.

In this study of YSZ3–Ni–YSZ3 assembly, voids are observed in the nickel side of the nickel oxide layer as shown in Fig. 5. This is consistent with other observations [4, 9–11] that the metal oxide becomes more porous at high temperature and hence voids develop in the nickel and nickel oxide interface.

Fig. 6 illustrates the effect of the bonding pressure on the shear strength of the bonding assembly bonded at 900°C for 15 min. A reduced load of 4.4 MPa is applied during cooling for bonding pressure greater than 4.4 MPa, while the same amount of load is employed as the bonding pressure if the bond-

ing pressure is less than 4.4 MPa. As seen from Fig. 6, the shear strength increases abruptly with the bonding pressure. There exists a threshold bonding pressure above which appreciable strength could be observed. In fact, the optimum bonding pressure depends on the bonding temperature, bonding time and the surface topography of the nickel and YSZ3 specimen. The higher bonding pressure gives more contacts between the nickel and the ceramics. It is believed that the adherent area between the metal and ceramics would increase as the bonding pressure is promoted. Higher shear strength is expected if the bonding pressure exceeds the value 8.17 MPa employed in this study, which is, however, limited by the current set-up for the test.

In order to study the effect of the bonding temperature on the strength, a series of bonding test was carried out at temperature 550 to 1100°C under the bonding pressure of 8.17 MPa for 15 min. A reduced load of 4.4 MPa is applied during cooling after bonding. Fig. 7 shows the temperature dependence of the bonding test. The bonding strength increases as the bonding temperature increases. It is generally believed that the surface energy is a crucial factor in the

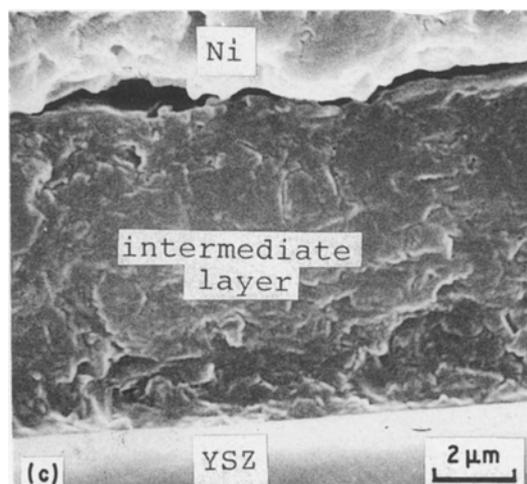
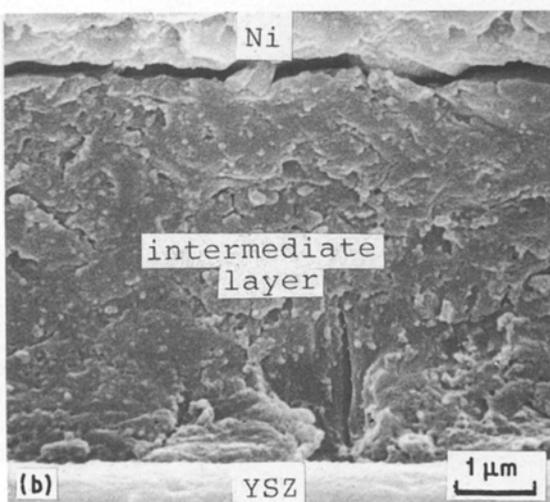
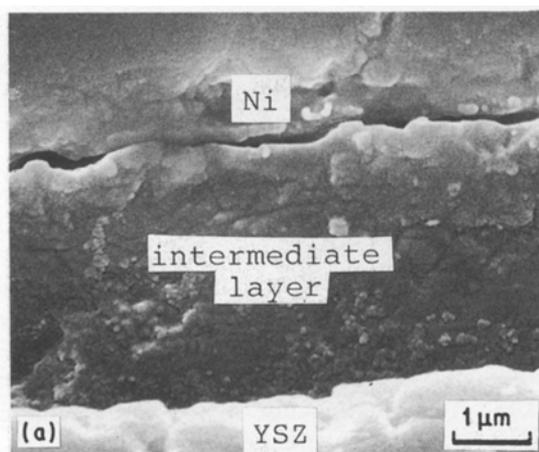
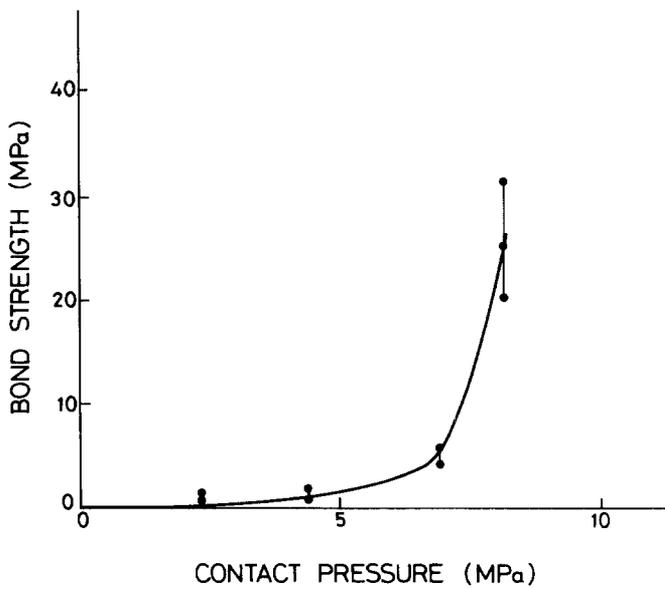


Figure 5 SEM micrographs of the bonding interfaces at 900°C under 8.17 MPa for various bonding time (a) 5 min, (b) 10 min, (c) 15 min.

Figure 6 The pressure dependence of the shear strength bonded at 900°C for 15 min.



ceramic-metal bonding mechanism and an Arrhenius relationship exists for the bonding strength and the bonding temperature [12].

According to the work of Yamane and coworkers [4], the temperature dependence is similar to the time dependence, in which voids are observed for longer bonding time and this results in a lower bond strength. Nevertheless, the bonding strength does not decrease when the temperature is up to 1100°C in this study. The main difference is attributed to the cooling process. In Yamane's work, the couples were taken out of the apparatus and then air cooled without any loading. While in this study a reduced load, usually 4.4 MPa, was employed. The application of the reduced load tends to compress the enlarging voids formed between the nickel and nickel oxide interface, and thus the bonding strength does not decrease at the high temperature. For the case of cooling without any loading, the accelerated growth of NiO at the high temperature and the introduced interstices at the interface would result in a decrease in the bonding strength.

The effect of cooling on the bond strength after bonding can be further appreciated by carrying out

the bond test with various cooling rates. It is observed that the shear strengths reduce to 7.1 and 12.3 MPa, respectively, for air cooling and furnace cooling without any loading, as compared to  $26 \pm 5$  MPa for 4.4 MPa loading after bonding. The introduction of loading after bonding leads to more intact interface and thus higher bonding strength.

### 3.2. The effect of pre-coating

The effect of pre-coated Ni on the bonding strength is investigated by carrying out the bond test with various coating thickness of Ni on the YSZ3 surface at 900°C under 8.17 MPa for 15 min. The pre-coating was conducted with a cold sputter coater (POLARON E5100, England). A reduced load of 4.4 MPa is applied during cooling after bonding.

Fig. 8 shows the dependence of the pre-coated Ni thickness on the shear strength of YSZ3-Ni-YSZ3 bonded at 900°C for 15 min under 8.17 MPa in air. The bonding strength increases sharply with the coating thickness at the initial stage. Between 1 μm and 1.5 μm, the bonding strength reaches a maximum value, and then it decreases as the coating thickness increases.

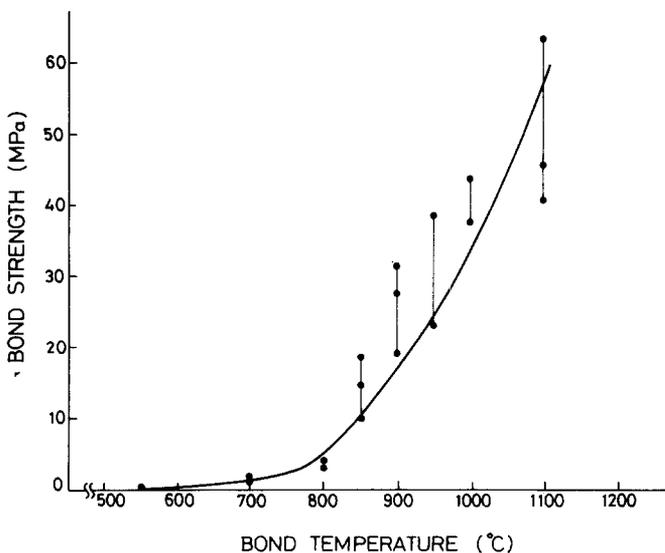


Figure 7 The temperature dependence of the shear strength bonded under 8.17 MPa for 15 min in air.

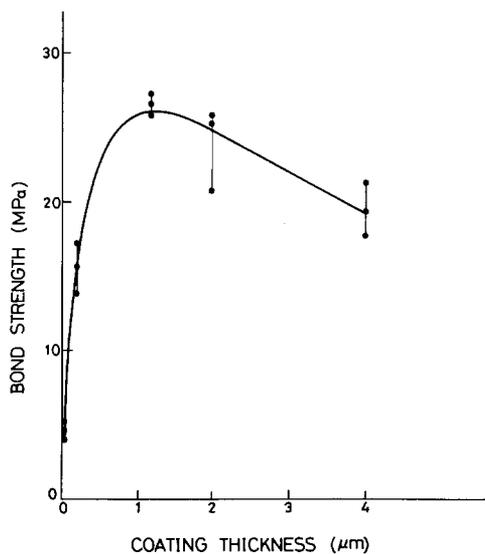


Figure 8 The dependence of the pre-coated thickness of Ni on the shear strength of YSZ3-Ni-YSZ3 at 900°C for 15 min.

Generally speaking, a thin coating is not sufficient to preserve a continuous and integral film with good adhesion between the coating and the underlying substrate. For pre-coated Ni thickness less than 100 nm in this study. It seems that a good adhesion between the pre-coating Ni and YSZ3 ceramics can not be obtained. In addition, the application of the pressure during bonding tends to introduce a tear force on the coated film and possibly reduces the contact area between Ni and YSZ3. As a result, the bonding strength for thin pre-coated bonding assembly is less than that without pre-coating, as shown in the Fig. 8.

Fig. 9 shows the SEM micrograph of the bonding interface for pre-coated 1.2 μm Ni on YSZ3 ceramics at 900°C under 8.17 MPa for 15 min. By comparing Fig. 9 with Fig. 5c, which is the result for the uncoated assembly bonded at the same condition, it seems that the thickness of NiO layer increases from 8.5 μm in Fig. 5c to 10 μm in Fig. 9. The difference of the NiO thickness between these two cases, 1.5 μm, results from the transformation of the pre-coated 1.2 μm Ni to the NiO layer in the intermediate region. This can be verified by taking into account the volume ratio

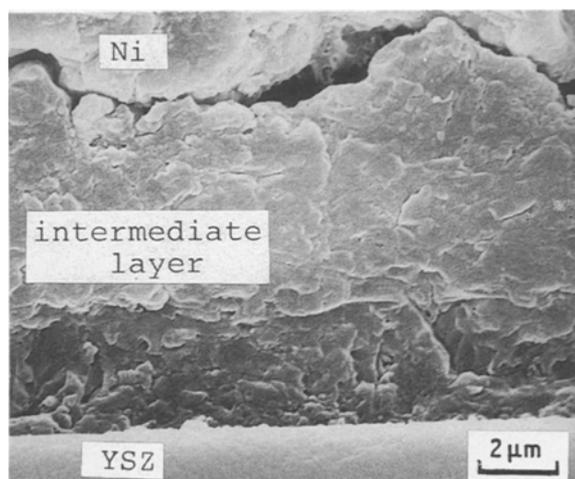


Figure 9 SEM micrograph of the bonding interface for pre-coated 1.2 μm Ni on the YSZ at 900°C under 8.17 MPa for 15 min.

between NiO and Ni, as follows.

$$\begin{aligned} & \text{pre-coated Ni thickness} \times \left( \frac{V_{\text{NiO}}}{V_{\text{Ni}}} \right)^{1/3} \\ &= \text{increase of NiO thickness due} \\ & \quad \text{to transformation from pre-coated Ni} \end{aligned}$$

where the volume ratio  $V_{\text{NiO}}/V_{\text{Ni}}$  is 1.65. The pre-coated Ni thickness 1.2 μm times the one third power of the volume ratio  $[(1.65)^{1/3}]$  is close to the increase of NiO thickness 1.5 μm, which is observed experimentally.

It is expected that the application of sufficient pre-coated Ni film would increase the contact area of the interface in the metal-ceramics bonding as the sputtered film tends to contour the originally polished YSZ3 surface. Thus, a relatively higher bonding strength is obtained as shown in Fig. 8 for the bonding assembly with pre-coated 1.2 μm Ni.

The thickness of the NiO layer in the bonding assembly at 900°C under 8.17 MPa for 15 min for pre-coated 4 μm Ni increases to 13.5 μm from the original 8.5 μm without coating. The increase of the NiO thickness, 5 μm, also comes from the transformation of pre-coated Ni to NiO layer, as discussed before by considering the volume ratio between the NiO and Ni. Because of the enhancement of the NiO layer, the introduced stress due to cooling would result in an increase of the interstices, which in turn causes the bonding strength to decline. The interstice size increases from 0.48 μm without coating to 1.8 μm with pre-coating [14]. As a consequence, the bonding strength decreases if the pre-coated Ni thickness exceeds a threshold thickness, whereas the negative effect of introduced stress due to enlarged NiO layer begins to predominate over the positive contribution of enhanced contact area due to the pre-coated film.

The result in Fig. 8 is not in total agreement with the work of Bailey's [4], in which an evaporated 300 nm Au was onto the Al<sub>2</sub>O<sub>3</sub> ceramics. It was reported that the pre-coating would significantly increase the bonding strength of Al<sub>2</sub>O<sub>3</sub>-Au-Al<sub>2</sub>O<sub>3</sub>. The bonding between Au and Al<sub>2</sub>O<sub>3</sub> is, in fact, a surface reaction type, in which the bonding strength mainly relies on the contact area between Au and Al<sub>2</sub>O<sub>3</sub>. In this study, the bonding between Ni and YSZ3 is, however, a diffusion related phenomenon and the development of the intermediate NiO layer plays an important role in the bonding strength besides the contact area consideration. In the system of YSZ3-Ni-YSZ3 bonding assembly, the bonding strength is determined by the compromise between the positive contribution of contact area and the negative contribution of the stress in the NiO layer.

#### 4. Conclusions

1. Sandwich-type assembly of YSZ3-Ni-YSZ3 is fabricated by solid state bonding. The shear strength reaches optimum values between 10 and 25 min at 900°C under a bonding pressure of 8.17 MPa.

2. The decrease of shear strength for longer bonding time is attributed to the introduced stress between the metal and the ceramics as well as the enlarged voids formed at the Ni-NiO interface.

3. The cooling process after bonding has influence on the measured shear strength. The application of a reduced load during cooling results in higher shear strength.

4. Pre-coating of Ni films on the YSZ ceramics affects the bonding strength of YSZ–Ni–YSZ. An optimum strength is obtained for the bonding assembly with 1–1.5  $\mu\text{m}$  pre-coated Ni film at 900° C for 15 min under 8.17 MPa.

### Acknowledgement

The authors thank the National Science Council, Taiwan for financial support under the contract No. NSC77-0405-E007-26R, and NSC77-0404-E009-30.

### References

1. H. J. DE BRUIN, A. F. MOODIE and C. E. WARBLE, *J. Mater. Sci.*, **7** (1972) 909.
2. A. J. KINLOCH, *J. Mater. Sci.* **15** (1980) 2141.
3. R. V. ALLEN, W. E. BORRIDGE and P. T. WHELAN, in "Science and Technology of Zirconia II", edited by N. Claussen, M. Rühle and A. H. Heuer (The American Ceramic Society, 1984) p. 537.

4. T. YAMANE, Y. MINAMINO, K. HIRAO and H. OHNISHI, *J. Mater. Sci.* **21** (1986) 4227.
5. J. T. KLOMP and A. J. C. VAN DE VEN, *J. Mater. Sci.* **15** (1980) 2483.
6. S. L. SHINDE and L. C. DE JONGHE, *J. Electron. Micro. Tech.* **3** (1986) 361.
7. Australian Pat. 452651, U.S. Pat. 4050956, CSIRO and the Flinders University, South Australia.
8. TSK Ceramics Technical Bulletin, Toyo Soda Manufacturing Co. LTD., No. Z-112 (1986).
9. R. HALES and A. C. HILL, *Corrosion Sci.* **12** (1972) 843.
10. G. C. WOOD, I. G. WRIGHT and J. M. FERGUSON, *Corrosion Sci.* **5** (1965) 645.
11. F. N. RHINES, R. G. CONNELL JR and M. S. CHOI, *J. Electrochem Soc.* **126** (1979) 1061.
12. J. T. KLOMP, in "Materials Research Society Symposium Proceedings vol. 40, edited by E. A. Giess, K. N. Tu and D. R. Uhlmann (Materials Research Society, U.S.A., 1985) p. 381.
13. F. P. BAILEY and K. J. T. BLACK, *J. Mater. Sci.* **13** (1978) 1045.
14. Y. C. WU, M.S. dissertation, National Tsing Hua University (1987).

*Received 20 March*

*and accepted 4 September 1989*